Influence of Perforation Angle and Infill Density on Sound Absorption Coefficient of 3D Printed Bio-degradable PLA Panel

Jipson GEORGE
Department of Mechanical Engineering, Government College of Engineering Kannur, India, jipsongeorge2015@gmail.com

Sudheesh KUMAR C P *
Department of Mechanical Engineering, Government College of Engineering Kannur, India, sudheeshkumar3@gmail.com

* Author to whom correspondence should be addressed

Abstract: - Noise pollution is a major environmental challenge that drives the need for sustainable sound-absorbing materials. Conventional absorbers are often derived from hazardous, non-biodegradable polymers, whereas polylactic acid (PLA) offers a non-toxic, biodegradable, and recyclable alternative. This study investigates the sound absorption coefficient (SAC) of 3D-printed, disc-shaped PLA panels with perforations. A detailed numerical analysis, using a virtual impedance tube in COMSOL Multiphysics software, along with experimental validations with the help of a real impedance tube are carried out. The influence of the thickness of the disc, infill ratio, and perforation angles on acoustic performance is systematically examined. Results indicate that both perforation angles and infill density significantly affect SAC. This helps in developing PLA discs for improved sound absorption while maintaining their lightweight, compact, and cost-effective designs. These findings establish PLA as a promising sustainable alternative to synthetic acoustic materials, offering new opportunities for eco-friendly noise control solutions in industrial and architectural applications.

Keywords: - sound absorption coefficient, PLA panel, perforation angle

1. INTRODUCTION

Noise pollution is the third most serious environmental hazard after air and water pollution, with proven links to hypertension, cardiovascular disease, and reduced quality of life. Conventional absorbers such as glass wool and polyurethane foams, while effective, are hazardous, non-biodegradable, and environmentally unsustainable. In response, polylactic acid (PLA), a non-toxic, biodegradable, and recyclable polymer, offers a promising green alternative for acoustic applications.

Sound-absorbing elements used for noise control applications are of different sizes and geometries. These are commonly disc-shaped, cone-shaped, pyramid-shaped, or wedge-shaped and are mounted on the room's interior walls in some specific patterns [1]. Many studies are being conducted to reduce the effect of sound by using various sound-absorbing elements. A study conducted by the World Health Organization says that noise pollution is considered the third most hazardous one after air and water pollution [2,3]. Exposure to large noise has an effect on humans, which can bring psychiatric disorders such as hypertension, anxiety, high blood pressure, etc. [4]. The major sources of sound in industries are pneumatic presses, forging, and drilling machines [5,6]. The materials used for sound-absorbing elements are generally of a porous type due to the presence of voids and cavities, which give obstruction to sound propagation and dissipate the energy of sound waves. These obstructions produce viscous loss to the propagating sound wave, which makes porous material work better in the application of sound acoustics [7]. Due to their properties like lightweight, efficiency in sound absorption, and easy management, porous materials are considered the best sound absorbers [8]. Numerous studies have demonstrated that porosity is an important component for sound absorption. The open pores are taken into account since they are the sole contributors to the absorption of incident sound [9]. When examining sound absorption mechanisms in materials, the number, size, and kind of pores are all important factors to be considered [10]. As the air gap thickness rises, the sound absorption coefficient (SAC) increases at the mid and higher frequencies. It is also found that as the air gap layer is moved closer to the sample surface, the sound absorption performance diminishes [11].

A recent study tells that there are variety of artificially developed materials which are used in sound absorption applications. The main advantage

of using synthetic material in sound absorption is that it offers great flexibility in machining, and a large variety of designs is possible [12]. The diameter of the fibre is the most important component in improving the sound absorption capacity of any fibrous material, because as the diameter of the fibre decreases, the porosity of the material increases, thus increasing the viscous friction on the incident sound wave. It has been reported that the fibre size of natural materials is larger than that of artificial sound-absorbing materials [13,14]. Glass fibres and glass wools are possibly more carcinogenic and cause cancer in humans compared to other synthetic sound absorption materials. These materials are hazardous and represent serious environmental and health risks [15]. They leach poisons and are non-biodegradable, causing disposal problems. When heated over 220 °C, polyurethane foams release harmful gases such as isocyanides, hydrogen cyanide, halogenated chemicals, and alkenes [16]. A study of numerous methodologies for determining the toxicity of gases produced during the combustion of polyurethane foam, as well as their physiological, biochemical, and fatal consequences on people, has been presented [17]. The fire-toxic effects of glass wool, rock wool, expanded polystyrene, phenolic, polyurethane, and polyisocyanurate foams under different fire circumstances have been investigated [18]. As a result, the development of biodegradable materials for sound absorption and sound transmission loss applications is of great importance.

An efficient and environmentally green material for sound absorption and sound transmission loss (STL) applications using biodegradable resin was proposed [19]. A significant number of studies were pursued in developing high-performance, sustainable meta-materials for building MPPs from natural resources [20]. PLA is a kind of polymer that has minimal to no impact on the environment due to its sustainable properties. It is a non-toxic, bio-degradable, recyclable polymer with a well-documented thermal history. Furthermore, its mechanical qualities and convenience of use are equivalent to those of other polymers. PLA may also be combined with a variety of other materials to improve its qualities. A study on the acoustic behaviour of 3D printed bio-degradable panels made of PLA stated that the sound absorption of panels with varying perforations cross-section is better than that of panels with perforations of uniform cross-section [21]. But those perforations were straight in the longitudinal (axial) direction and did not have any inclination. PLA-based natural fibre composites made using 3D printing technology can be used for acoustic applications because they can create structures with different characteristics that absorb sound at different wavelengths. Another important feature of 3D printing is that its cost and time can be adjusted by varying the infill density [22].

Infill density is the "fullness" of a part's interior. In slicers, this is typically described as a percentage from 0 to 100, with 0% indicating a hollow component and 100% indicating a totally solid component [23]. Performance of acoustic panels of PLA reinforced wood fibre composites made by 3D printing was tested for different infill densities and thicknesses using a 2-microphone impedance tube, and the effect of shifting the frequency at which maximum sound absorption takes place was reported [24]. However, those panels were made of reinforced wood fibre composites and were tested with air gaps.

Recent advances in 3D-printed and natural fiber–reinforced PLA composites have shown strong potential for acoustic applications. Studies demonstrated that 3D-printed PLA panels with smaller nozzle diameters (0.4 mm) enhanced sound absorption (α up to 0.91), whereas larger nozzles (0.8 mm) improved sound transmission loss (STL up to 56 dB) through geometric optimization [27]. PLA–cork fiber micro-perforated panels (MPPs) achieved 25% higher absorption than conventional MPPs, with optimal performance at 0.70 mm perforation diameter, 0.90 mm thickness, and 8 mm spacing, further improved with kenaf layers [28]. PLA foam–plant fiber composites (grape stems, wood straw) exhibited better performance than pure PLA above 1500 Hz, while also reducing cost and environmental impact [29]. Coffee waste/PLA MPPs achieved peak absorption of 0.90 at 800 Hz and reduced reverberation time by 0.59 s at 1000 Hz, providing sustainable café noise control [30]. Eco-friendly PLA composites reinforced with water hyacinth and pineapple leaf fibers achieved strong mechanical and acoustic performance, with a maximum sound absorption value of 0.55 at 5000 Hz (WHF/PLA) and 0.83 at 4000 Hz (PALF/PLA), along with tensile strength about three times higher than non-3D-printed versions [31].

A review of natural fiber–reinforced PLA composites highlighted the influence of fiber type, porosity, and geometry, while noting emerging strategies such as nano-coatings, hybrid structures, and 3D printing for enhanced acoustic materials [32]. Beyond experimental work, a radial basis function (RBF) neural network model for open-cell aluminum foams achieved a minimum mean root mean square error (RMSE) of 0.012 and maximum RMSE of 0.023, outperforming classical Delany–Bazley (0.121) and Johnson–Champoux–Allard (0.097) models for low- and mid-frequency

predictions [33]. Open-porous PLA structures with porosities of 30–56% and thicknesses of 10–30 mm revealed that higher porosity (56%) and thinner samples (10 mm) improved reflection (β ≈ 0.9), while increased thickness reduced low-frequency performance [34]. PLA, high-impact polystyrene (HIPS), and polyethylene glycol (PETG) panels showed that PLA reduced sound pressure by approximately 30 dB (95.8 → 65.8 dB, approximately 45%) at 10 kHz, while PETG achieved losses up to 26.6 dB, with frequency (approximately 13 kHz) [35]. Auxetic PLA structures reinforced with chicken keratin exhibited superior absorption, with rachis-reinforced composites reaching α = 1.126 (1/mm) at 5 kHz, compared to plain auxetic PLA (0.823) and honeycomb PLA (0.739), confirming keratin's significant role in enhancing acoustic performance [36].

From the literature, a few papers on the sound absorption characteristics of acoustic panels made of PLA can be seen. However, the effect of perforation angles and the infill densities on the acoustic behavior of panels made of PLA has not been reported.

2. METHODOLOGY

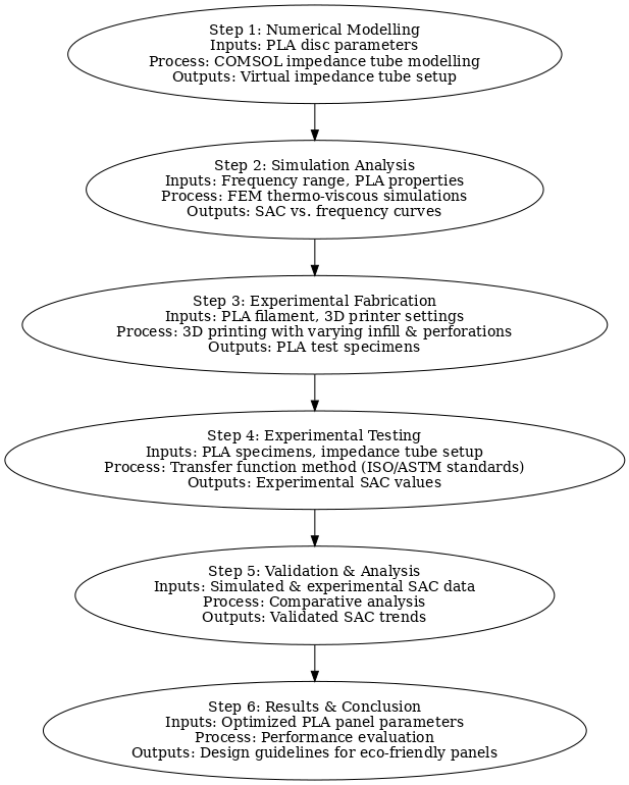

Figure 1. Flow chart showing the methodology

The methodology mainly consists of six different stages, namely modeling, numerical analysis, fabrication, testing, validation, and results and conclusion, as described in Figure 1. First of all, for analyzing the sound absorption characteristics of PLA material, a computational model is developed using COMSOL Multiphysics software. The analysis is performed to examine the influence of perforation angle, plate thickness, and infill density on the sound absorption coefficient. Following this, experiments are carried out using 3D-printed PLA plates of 10,15and 20 mm thickness with perforation angles of 0°, 60°, and 75°, and infill densities of 50%, 75%, and 100%, tested in an impedance tube under ASTM standards.

Table 1. Properties of Polylactic acid [21]

Specific gravity	1.25
Relative viscosity	3.30
Melting point (°C)	190 - 230
Yield strength, Tensile (MPa)	63
Elongation (%)	3.6

2.1. Numerical Method

2.1.1. Modelling of impedance tube

A virtual 3D impedance tube is modelled using COMSOL Multiphysics 5.6 to estimate the sound absorption coefficient (SAC). It is modelled using thermos-viscous acoustic module to account for both viscous and thermal losses. The tube has a circular cross-section of 100 mm diameter and 900 mm length, with two microphones placed at a spacing of 150 mm. The main specifications of the impedance tube are given in Table 2, and Figure 2 shows the virtual impedance tube, which is modelled using COMSOL Multiphysics software. It can be seen that x_1 is the distance between the first microphone and the wedge tip, p_1 and p_2 are the total sound pressures at the first and second microphones, respectively.

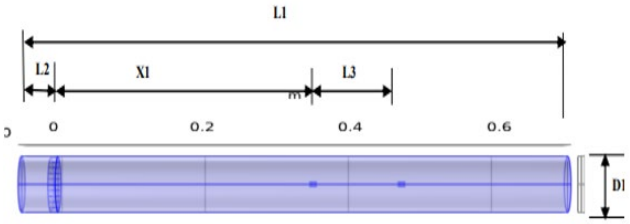

Figure 2. Virtual impedance tube modelled in COMSOL

2.1.2. Modelling of PLA discs

A disc-shaped sound absorbing element with the parameters given in Tables 1-3, having perforations of different angles (0°, 15°, 45°, 60°), is modelled.

Table 2. Impedance tube dimensional parameters

L1	900 mm	Length of tube
D1	100 mm	Cross-sectional diameter
L2	200 mm	Length of air gap
L3	150 mm	Microphone spacing

A disc with a 100 mm diameter is shown in Figure 3. Models having thicknesses of 10 mm, 15 mm, and 20 mm are also modelled for a 0˚ perforation angle.

Table 3. Specifications of disc element [21]

Material	Polylactic acid
Thickness of plate	10 mm
Diameter of plate	100 mm
Perforation diameter	1 mm

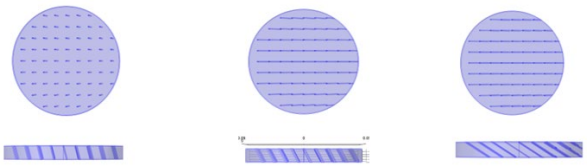

a *b* *c*

Figure 3. Plate with different perforation angles: (a) 15°, (a) 45° and (a) 60°

2.1.3. Analysis

The numerical simulation using COMSOL provides SAC values for different specimen geometries. The analysis is carried out over a frequency range of 300–5000 Hz. The standards followed for the simulation are ISO10534-2 and ASTM C384. Plane waves are generated at one end of the virtual impedance tube. A background pressure of 1 Pa is applied in the pressure field domain. Material properties assigned to the model are directly imported from the built-in library.

Finite element meshing is applied with a mesh size determined by the wavelength of the maximum frequency. The finite element mesh size is chosen based on the wavelength corresponding to the highest frequency given by Eq. (1).

$$\lambda_{min} = \frac{C_o}{f_{max}} \quad (1)$$

where C_o is the speed of sound and f_{max} is the maximum frequency in the model. The higher frequency (f_u) and the lower frequency (f_l) of the tube and the distance between the two microphones (s) are calculated from Eqns. (2-4).

$$f_u d < 0.5 C_o \quad (2)$$

$$f_l > \frac{0.75 C_o}{l-d} \quad (3)$$

$$f_u s < 0.45 C_o \quad (4)$$

where l is the overall length of the tube, and d is the diameter of the tube. Also, the distance between the two microphones should be greater than 5% of the longest wavelength, which is the lowest frequency of interest. Thermo-viscous acoustic simulations are employed to account for both viscous and thermal energy losses. The SAC is calculated using Eq. 5.

$$\text{SAC} = 1 - |\text{Rc}|^2 \quad (5)$$

where the reflection coefficient Rc = Pr/Pi, in which the incident pressure (P_i) and the reflected pressure (P_r) are obtained in post-processing.

2.2. Experimental Method

2.2.1. Preparation of samples

Test samples are fabricated using the fusible deposit method (FDM) in a 3D printer. Physical and material properties of PLA used in 3D printing are given in Tables 1-3. Circular discs are prepared with three infill densities (50%, 75%, and 100%) having perforation angles of 0°, 60°, and 75°, and diameters of 29 mm and 100 mm to suit the impedance tube holders Figure 4. Printing is performed with a 0.4 mm nozzle, 0.2 mm layer height, 55 mm/s speed, at a nozzle temperature of 210 °C, and bed temperature of 60 °C. Environmental conditions of 20 °C with no moisture are maintained to ensure good print quality.

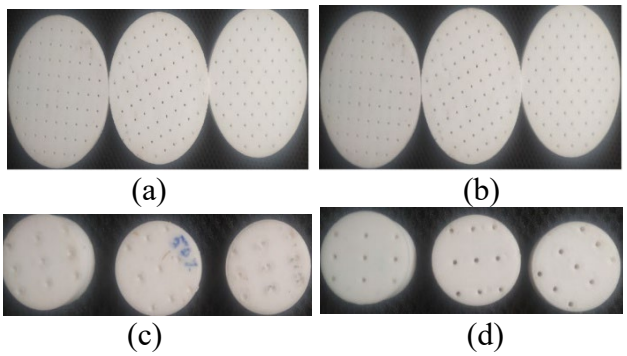

(a) (b) (c) (d)

Figure 4. 3D printed PLA plate (a) & (b) 100 mm diameter plate, (c) & (d) 29 mm diameter plate

2.2.2. Sound absorption tests

The fabricated specimens are tested in an anodized aluminium impedance tube equipped with a loudspeaker and two microphones, conforming to ISO 10534-2, ASTM E1050, and ASTM E2611 standards. The transfer function method is employed to calculate SAC by separating incident and reflected sound waves. The frequency range is 100–6300 Hz, which depends on the inner tube diameters of 29 mm or 100 mm. The impedance tube shown in Figure 5 is made of anodized aluminium and is meant to evaluate sound absorption coefficient and transmission loss according to ISO 10534-2, ASTM E1050, and ASTM E2611 test standards at normal incidence, that is, 0°. The test sample's acoustic properties are estimated using the transfer function

approach, which separates incident and reflected energy from the measured transfer function.

Table 4. Specifications of the impedance tube

Model No	HO-AE-ITA219
Tube	Combined type (Large 100 mm & Small 29 mm)
Inner Diameter	100 mm 29 mm
Frequency Range	100Hz - 1600 Hz 500Hz - 6300Hz
Sample Holder	100 mm 29 mm
Sample Holder	200 mm 200 mm
Standard	ISO10534-2, ASTME1050, ASTME2611
Loud Speaker	3½ "in diameter, 30 Watts, 4 Ohm
Microphone	¼" in diameter, -3dB at 1.5V sensitivity, 20-16,000Hz frequency response
Measurement software	Holmarc Wave Analyzer 4C
Measured parameter	Sound Absorption Coefficient (α)

Figure 5. Impedance tube

2.3. Validation

The experimental results are compared with the numerical results obtained from the virtual impedance tube (COMSOL Multiphysics). First of all, the results obtained from the simulation (Figure 7) using COMSOL are validated with the available experimental result [21]. The perforations in the plate are straight and are of uniform cross-section. The maximum value of the sound absorption coefficient obtained by simulation is 0.91, which is close to the experimentally obtained value of 0.94. The percentage of error between the two methods is about 3.2%, though there is a frequency shift of around 170 Hz between the peak values of the two results. This shift could be due to the mounting conditions in the impedance tube [25] and the ideal conditions in the software.

Figure 6. 3D printed plate with 50%, 75% and 100% infill density

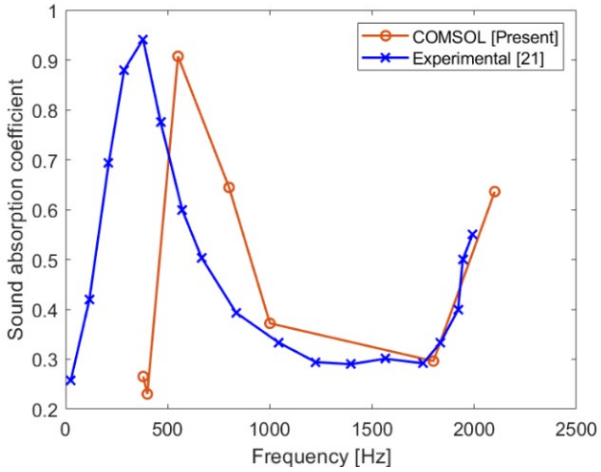

Figure 7. Sound absorption coefficients for PLA discs with straight and uniform cross-sections

2.4. Influence of different parameters on SAC

Having validated the numerical results with experimental data, the simulation is extended to different cases to investigate the influences of i) perforation angle, ii) plate thickness, and iii) infill density on the sound absorption coefficients. This is done to identify the optimal parameters that maximize the SAC.

2.4.1 Perforation angles

The influence of perforation angle on the sound absorption coefficient (SAC) is illustrated in Figure 8. Although the maximum SAC of 0.9 at 550 Hz remains unaffected by perforation angle, increasing the angle enhances absorption at other frequencies. Quantitatively, at low frequencies

below 1000 Hz and above 2000 Hz, discs with all perforations show almost the same SAC, while in the mid frequency range (1000-2000 Hz) the 60° perforated disc shows higher SAC compared to the 15 and 45 perforated discs.

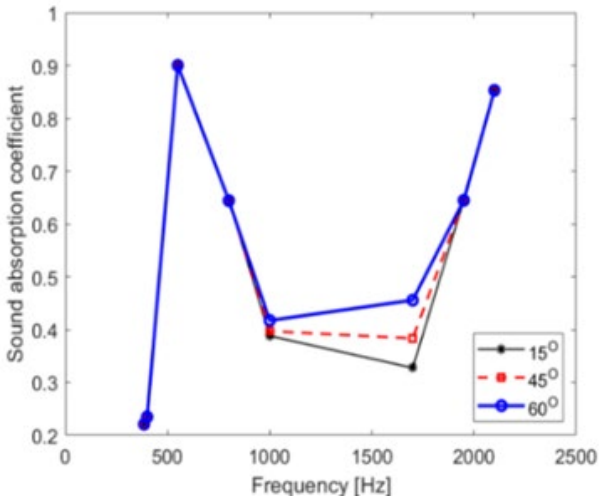

Table 4: Specifications of impedance tube

From Table 5, the maximum variation occurs at 1650 Hz, where the SAC of inclined perforations shows a substantial increase compared to straight (0°) perforations, with the 60° configuration providing the greatest improvement. This enhancement is attributed to the longer path length of sound waves within the porous region at higher angles, which increases viscous resistance and energy dissipation.

Table 5. Percentage change of sound absorption coefficient with perforation angle

Sl. No	Perforation Angle (°)	Frequency (Hz)	Percentage increase in α
1	15°	1650	10 %
2	45°	1650	34 %
3	60°	1650	54 %

As observed, though the increase in perforation angle does not change SAC, the corresponding frequency SACs at other frequencies are considerably improved. The physics behind this phenomenon is simple. As illustrated in Figure 9, increasing the perforation angle causes the sound waves to travel a greater distance and dissipate more energy so as to get more sound energy absorbed within the panel, which is almost the same as increasing the panel thickness. The effect of changing the perforation angle on the SAC of panels made of PLA has not been reported. So, instead of increasing the thickness of the panels, the perforation angle can be increased so as to have a minimum panel thickness, weight, and cost. These findings in the present work will enable the design of low-cost, light-weight, and compact panels for sound absorption.

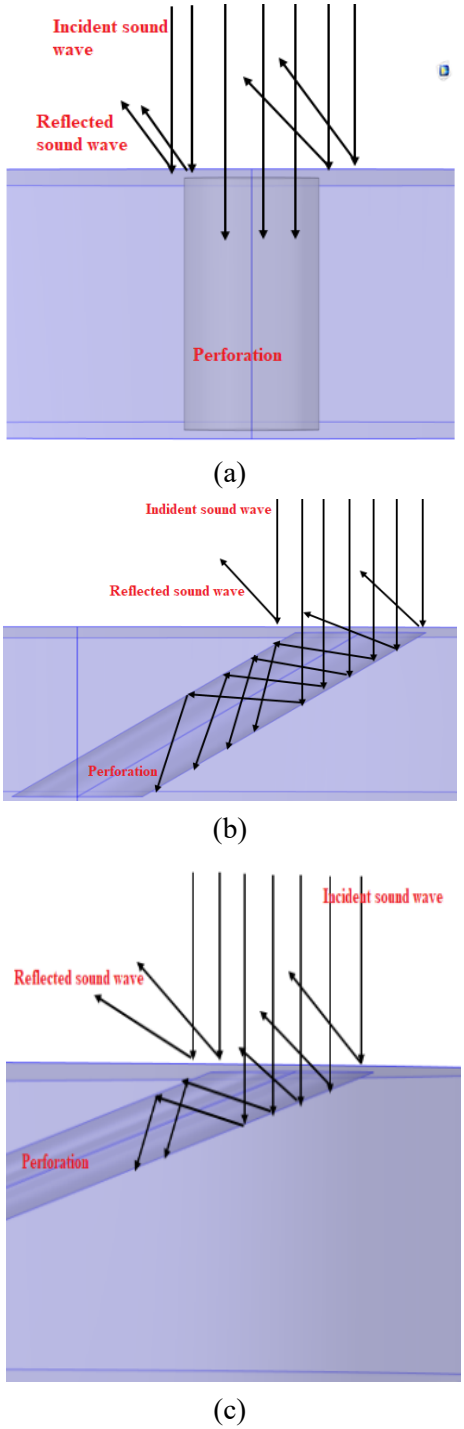

Figure 9. Perforation angles (a) 0 ^{o} (b) 60^{o}, and (c) 75^{o}

2.4.2. Plate thickness

In this part, the influence of plate thickness on the sound absorption coefficient (SAC) of perforated PLA discs is studied. Fig 10 and Table 6 show the results for three thicknesses (10 mm, 15 mm, and 20 mm) with 0° perforation angle. Similar to the case of perforation angles, increasing thickness does not alter the maximum SAC, which remains at ≈0.92 at

550 Hz for all cases. However, the thickness significantly influences the performance at other frequencies, with the most notable variation occurring at 1700 Hz. Table 6 indicates an almost 92% increase in SAC for the 20 mm disc compared to the 10 mm disc. In the mid-frequency range (1000–1500 Hz), the 10 mm sample exhibits the lowest SAC (around 0.3), while thicker specimens (15 mm and 20 mm) maintain higher absorption levels (0.4–0.5). At higher frequencies (around 2000 Hz), the absorption improves with thickness, with the 20 mm disc reaching SAC of around 0.85, outperforming the 15 mm and 10 mm discs. These results confirm that while thickness does not affect the peak low-frequency absorption, it plays a crucial role in enhancing absorption at mid- and high frequencies.

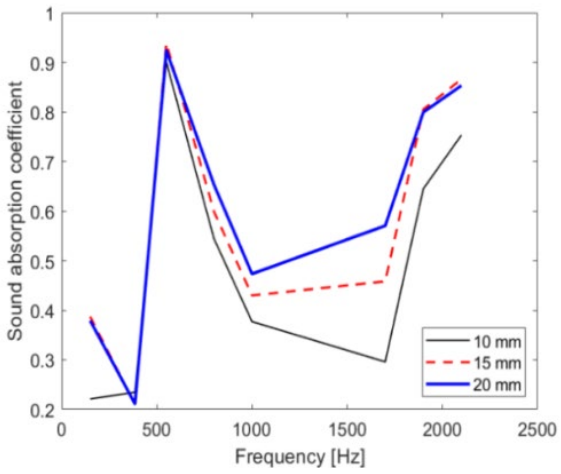

Figure 10. Effect of plate thickness on SAC

Table 6. Percentage change of sound absorption coefficient with plate thickness

Sl. No	Plate thickness (mm)	Frequency (Hz)	Percentage increase in α
1.	10	1700	-
2.	15	1700	54 %
3.	20	1700	92 %

2.4.3. Infill density

Infill density is an important parameter that influences both the energy-absorbing properties of 3D-printed structures and their manufacturing cost and time. Lowering the infill density introduces more void spaces inside the panel, which enhances viscous friction and leads to greater dissipation of acoustic waves, thereby improving sound absorption. In this work, panels with three different infill densities (50%, 75%, and 100%) are tested.

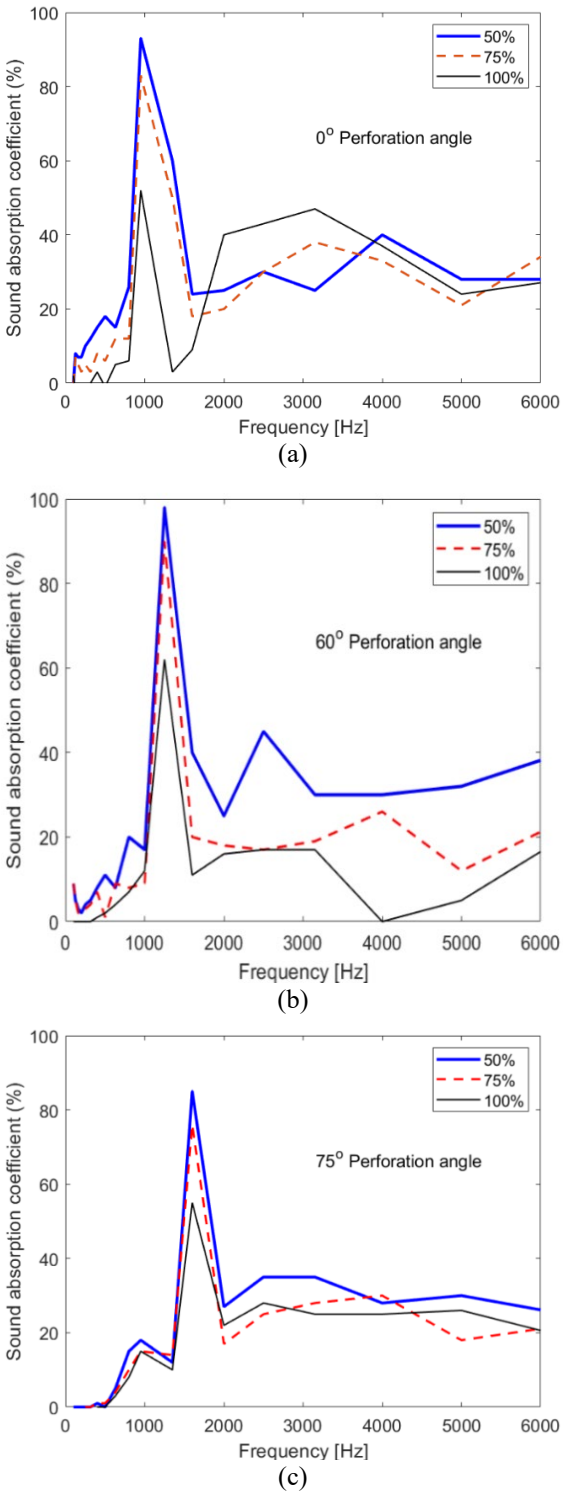

Figure 11. SAC at different infill densities (a) 0° (b) 60° and (c) 75° perforation angle

From Figure 11 and Table 7, it is observed that at a 0° perforation angle, the maximum sound absorption is achieved at 50% infill density. As the infill density increases, the peak value of the sound absorption coefficient is found to decrease. This is because higher density creates smaller pores in the interior of the plate, restricting the passage of low-frequency sound waves and causing a larger portion of the energy to be reflected at the surface [26].

Table 7. Maximum sound absorption coefficient (α) at a different angle of perforation

Infill density (%)	Perforation angle (°)	Frequency (Hz)	Peak SAC (α)	% Change
50	0	950	93	-
	60	1350	98	5.4
	75	1600	88	-5.4
75	0	950	83	-
	60	1350	90	8.4
	75	1600	76	-15.6
100	0	950	52	-
	60	1350	62	19.2
	75	1600	55	-11.3

At 0°, the maximum SAC appears near 1000 Hz, with the 50% infill plate reaching almost 90% absorption. At 60°, the peak remains near 1000 Hz, where the disc with 50% infill density again performs the best, achieving nearly 100% absorption, while higher infill percentages show significantly weaker performance. At 75°, the peak shifts to around 1500 Hz, with the 50% infill plate again showing the highest absorption (~85%), while the 75% and 100% plates provide moderate but lower values. Beyond the peak corresponding to maximum SAC, the 50% infill plate consistently delivers stronger and more stable absorption (30–40%) across the mid-to-high frequency ranges, whereas the 75% and 100% infill plates offer relatively weaker but steadier absorption. Overall, the 50% infill configuration demonstrates superior absorption performance at all perforation angles

3. CONCLUSION

Sound absorption characteristics of a perforated PLA disc are investigated in this paper. While most of the work is numerical simulation using COMSOL Multiphysics software, an experiment is also carried out for validation purposes. The results show that perforation angle, thickness, and infill density significantly influence the sound absorption coefficient (SAC) of PLA panels. Numerical results show that increasing the perforation angle from 0° to 60° enhances the SAC by up to 5.4% (93% to 98%) at 1350 Hz, while it gets reduced by 10.2% (98% to 88%) with further increasing the perforation angle to 75°. So, for 50% infill density, the optimal perforation angle is 60°. It is found to be the same (from Table 7) for other infill densities as well. These results show that the larger the perforation angles improve dissipation by lengthening the sound path, while increased thickness enhances absorption in the mid- and high-frequency ranges.

Plate thickness is also an influencing parameter, with a 92% increase in SAC at 1700 Hz when the thickness is raised from 10 mm to 20 mm

Increasing infill density is found to decrease the sound absorption coefficient because higher density creates smaller pores in the interior of the plate, restricting the passage of low-frequency sound waves and causing a larger portion of the energy to be reflected at the surface [26]. Infill density of 50% infill exhibits the highest SAC (0.98 at 1350 Hz), whereas denser structures (100% infill) show reduced absorption (0.62 at 1350 Hz), showing that increased porosity enhances viscous dissipation.

Overall, an optimized PLA panel with 60° perforation angle, 20 mm thickness, and 50% infill provided the best balance of high absorption (up to 0.98), lightweight structure, and reduced material cost, demonstrating that biodegradable PLA can serve as an efficient and sustainable alternative to conventional synthetic absorbers.

REFERENCES

[1] K. C. Opiela, T. G. Zieliński, T. Dvorák, and S. Kúdela Jr., Perforated closed-cell aluminium foam for acoustic absorption, Applied Acoustics, vol. 174, p. 107706, Mar. 2021, doi: 10.1016/j.apacoust.2020.107706.

[2] C. Terry, M. Rothendler, L. Zipf, M. C. Dietze, and R. B. Primack, Effects of the COVID-19 pandemic on noise pollution in three protected areas in metropolitan Boston (USA), Biological Conservation, vol. 256, p. 109039, Apr. 2021, doi: 10.1016/j.biocon.2021.109039.

[3] B. Basu et al., Investigating changes in noise pollution due to the COVID-19 lockdown: The case of Dublin, Ireland, Sustainable Cities and Society, vol. 65, p. 102597, Feb. 2021, doi: 10.1016/j.scs.2020.102597.

[4] Z. U. R. Farooqi et al., Assessment of noise pollution and its effects on human health in industrial hub of Pakistan, Environ Sci Pollut Res, vol. 27, no. 3, pp. 2819–2828, Jan. 2020, doi: 10.1007/s11356-019-07105-7.

[5] Z. Y. Lim, A. Putra, M. J. M. Nor, and M. Y. Yaakob, Sound absorption performance of natural kenaf fibres, Applied Acoustics, vol. 130, pp. 107–114, 2018, doi: https://doi.org/10.1016/j.apacoust.2017.09.012.

[6] K. Dong and X. Wang, Development of cost effective ultra-lightweight cellulose-based sound absorbing material over silica sol/natural fiber blended substrate, Carbohydrate Polymers, vol. 255, p. 117369, Mar. 2021, doi: 10.1016/j.carbpol.2020.117369.

[7] Z. Du et al., The sound absorption properties of highly porous silicon nitride ceramic foams, Journal of Alloys and Compounds, vol. 820, p. 153067, 2020, doi: https://doi.org/10.1016/j.jallcom.2019.153067.

[8] Y. Fei et al., Extrusion Foaming of Lightweight Polystyrene Composite Foams with Controllable Cellular Structure for Sound Absorption Application, Polymers, vol. 11, no. 1, Art. no. 1, Jan. 2019, doi: 10.3390/polym11010106.

[9] Y. Fang, X. Zhang, and J. Zhou, Acoustic porous metasurface for excellent sound absorption based on wave manipulation, Journal of Sound and Vibration, vol. 434, pp. 273–283, 2018, doi: https://doi.org/10.1016/j.jsv.2018.08.003.

[10] X. Yang, X. Shen, H. Duan, X. Zhang, and Q. Yin, Identification of Acoustic Characteristic Parameters and Improvement of Sound Absorption Performance for Porous Metal, Metals, vol. 10, no. 3, Art. no. 3, Mar. 2020, doi: 10.3390/met10030340.

[11] T. G. Zieliński, R. Venegas, C. Perrot, M. Červenka, F. Chevillotte, and K. Attenborough, Benchmarks for microstructure-based modelling of sound absorbing rigid-frame porous media, Journal of Sound and Vibration, vol. 483, p. 115441, Sep. 2020, doi: 10.1016/j.jsv.2020.115441.

[12] L. S. Liang, X. L. Wu, N. N. Ma, J. J. Du, and M. B. Liu, The Sound Absorption Properties Comparison of Metal Foams and Flexible Cellular Materials, Materials Science Forum, vol. 933, pp. 357–366, 2018, doi: 10.4028/www.scientific.net/MSF.933.357.

[13] Y. Chen et al., A novel sound absorbing material comprising discarded luffa scraps and polyester fibers, Journal of Cleaner Production, vol. 245, p. 118917, Feb. 2020, doi: 10.1016/j.jclepro.2019.118917.

[14] S. Xie, S. Yang, C. Yang, and D. Wang, Sound absorption performance of a filled honeycomb composite structure, Applied Acoustics, vol. 162, p. 107202, May 2020, doi: 10.1016/j.apacoust.2019.107202.

[15] Z. Yan, K. Feng, J. Tian, and Y. Liu, Effect of high titanium blast furnace slag on preparing foam glass–ceramics for sound absorption, J Porous Mater, vol. 26, no. 4, pp. 1209–1215, Aug. 2019, doi: 10.1007/s10934-019-00722-0.

[16] M. Raj, S. Fatima, and N. Tandon, 'An experimental and theoretical study on environment-friendly sound absorber sourced from nettle fibers', Journal of Building Engineering, vol. 31, p. 101395, Sep. 2020, doi: 10.1016/j.jobe.2020.101395.

[17] J. Lee and I. Jung, Tuning sound absorbing properties of open cell polyurethane foam by impregnating graphene oxide, Applied Acoustics, vol. 151, pp. 10–21, 2019, doi: https://doi.org/10.1016/j.apacoust.2019.02.029.

[18] J. Su, L. Zheng, and Z. Deng, Study on acoustic properties at normal incidence of three-multilayer composite made of glass wool, glue and polyurethane foam, Applied Acoustics, vol. 156, pp. 319–326, Dec. 2019, doi: 10.1016/j.apacoust.2019.07.016.

[19] S. K. Sharma, S. R. Shukla, and A. K. Sethy, Acoustical behaviour of natural fibres-based composite boards as sound-absorbing materials, J Indian Acad Wood Sci, vol. 17, no. 1, pp. 66–72, Jun. 2020, doi: 10.1007/s13196-020-00255-z.

[20] F. Bucciarelli, G. P. Malfense Fierro, and M. Meo, A multilayer microperforated panel prototype for broadband sound absorption at low frequencies, Applied Acoustics, vol. 146, pp. 134–144, Mar. 2019, doi: 10.1016/j.apacoust.2018.11.014.

[21] R. Sailesh, L. Yuvaraj, J. Pitchaimani, M. Doddamani, and L. B. Mailan Chinnapandi, Acoustic behaviour of 3D printed bio-degradable micro-perforated panels with varying perforation cross-sections, Applied Acoustics, vol. 174, p. 107769, Mar. 2021, doi: 10.1016/j.apacoust.2020.107769.

[22] R. Srinivasan, W. Ruban, A. Deepanraj, R. Bhuvanesh, and T. Bhuvanesh, Effect on infill density on mechanical properties of PETG part fabricated by fused deposition modelling, Materials Today: Proceedings, vol. 27, pp. 1838–1842, 2020, doi: https://doi.org/10.1016/j.matpr.2020.03.797.

[23] J. Podroužek, M. Marcon, K. Ninčević, and R. Wan-Wendner, Bio-Inspired 3D Infill Patterns for Additive Manufacturing and Structural Applications, Materials, vol. 12, no. 3, Art. no. 3, Jan. 2019, doi: 10.3390/ma12030499.

[24] A Sekar, Vignesh, et al., Effect of thickness and infill density on acoustic performance of 3D printed panels made of natural fiber reinforced composites, Journal of Natural Fibers (2021): 1-9.

[25] Horoshenkov, Kirill V., et al., Reproducibility experiments on measuring acoustical properties of rigid-frame porous media (round-robin tests), The Journal of the Acoustical Society of America 122.1 (2007): 345-353.

[26] Qui, Hua, and Yang Enhui, Effect of thickness, density and cavity depth on the sound absorption properties of wool boards, Autex Research Journal 18.2(2018):203-208.

[27] S. Matei, M. A. Pop, S.-M. Zaharia, M. Cosniță, C. Croitoru, C. Spîrchez, and C. Cazan, Investigation into the Acoustic Properties of Polylactic Acid Sound-Absorbing Panels Manufactured by 3D Printing Technology: The Influence of Nozzle Diameters and Internal Configurations, Materials, vol. 17, no.3, p.580, Jan. 2024.

[28] E. Rezaieyan, E. Taban, U. Berardi, S. B. Mortazavi, M. Faridan, and E. Mahmoudi, Acoustic properties of natural fiber reinforced composite micro-perforated panel (NFRC-MPP) made from cork fiber and polylactic acid (PLA) using 3D printing, Journal of Building Engineering, vol. 84, p. 108491, Jan. 2024.

[29] F. Rotini, L. Fiorineschi, L. Conti, and G. Rossi, Investigating Polylactic Acid Foam–Plant Fiber Composites for Sound Absorption and Insulation, Sustainability, vol. 16, no. 16, p. 6913, Aug. 2024.

[30] S. T. Kang, J. Y. Choi, Y. U. Kim, and S. Kim, Acoustic performance of coffee waste/polylactic acid composite microperforated panels for noise control in cafe spaces, Building and Environment, vol. 279, p. 113062, 2025.

[31] N. K. Wijekoon, G. A. Appuhamillage, R. S. Dassanayake, R. N. Liyanage, D. Mapage, A. Wijenayake, E. L. Lokuge, S. M. Rajapaksha, G. A. Abeygunawardane, and N. D. D. Senarath, Facile fabrication of 3D-printed cellulosic fiber/polylactic acid composites as low-cost and sustainable acoustic panels, Sustainable Chemistry for the Environment, vol. 8, p. 100168, Oct. 2024.

[32] W. He, H. Tang, Z. Tang, W. Zhang, Y. Yang, and H. Li, Sound absorption performance of 3D printed porous polylactic acid materials with gradient distribution, Applied Acoustics, vol. 198, p. 109236, Mar. 2023.

[33] L. Liang, H. Mi, W. Guo, Y. Zhang, H. Ma, Z. Zhang, and L. Li, Estimation of sound absorption coefficient of composite structured aluminum foam by radial basis function neural network, Applied Acoustics, vol. 185, p. 108414, 2022.

[34] K. Monkova, M. Vasina, P. P. Monka, J. Vanca, and D. Kozak, "Effect of 3D-Printed PLA Structure on Sound Reflection Properties," Polymers, vol. 14, no. 3, p. 413, Jan. 2022.

[35] A. Hrituc, A. M. Mihalache, O. Dodun, G. Nagît, I. Besliu-Băncescu, B. Rădulescu, and L. Slătineanu, Propagation of Sounds through Small Panels Made of Polymer Materials by 3D Printing, Polymers, vol. 16, no. 1, p. 5, Dec. 2023.

[36] V. Amaya-Amaya, M. de Icaza-Herrera, A. L. Martínez-Hernández, G. Martínez-Barrera, and C. Velasco-Santos, Experimental approximation of the sound absorption coefficient ($\propto$) for 3D printed reentrant auxetic structures of polylactic acid reinforced with chicken keratin materials, Materials Letters, vol. 283, p. 128757, 2021.